

Multi-objective economic dispatch with residential demand response programme under renewable obligation

Thabo G. Hlalele^{a,*}, Jiangfeng Zhang^b, Raj M. Naidoo^a and Ramesh C. Bansal^c

^aDepartment of Electrical, Electronic and Computer Engineering, University of Pretoria, Pretoria, 0002, South Africa

^bDepartment of Automotive Engineering, Clemson University, Greenville, SC, 29607, USA

^cDepartment of Electrical Engineering, University of Sharjah, Sharjah, United Arab Emirates

*Correspondence to: greg.hlalele@gmail.com

Highlights

- Economic dispatch and demand response models are combined for renewable obligation.
- Real data from a large-scale direct load control programme are applied.
- Cost reductions are 21.57% and 15.81%, respectively, for two testing systems.

Abstract

This paper presents a combined economic dispatch and demand response optimisation model under renewable obligation. Real data from a large-scale demand response programme are used in the proposed model. The model uses renewable obligation policy and direct load control to find an optimal energy and reserve strategy that minimises generation costs and maximising renewable penetration. The real data from the South African large-scale demand response programme are used in which the system operator can directly control the participation of electric water heaters at the substation level. The actual load before and after demand reduction are used to assist the system operator in making optimal decisions on whether a substation should participate on the demand response programme. The application of real data to the proposed model avoids the traditional approaches which assume arbitrary controllability of flexible demand. The effectiveness of the model is tested using the modified IEEE 30 and 118-bus systems. The results show that the proposed model can achieve significant demand reduction as high as 830 MW for the IEEE 30-bus system and shift up to 401 MW. Moreover, a total cost reduction of 21.56% can be achieved using the IEEE 118-bus system.

Keywords: Dynamic economic dispatch; Demand response programme; Flexible demand; Residential load management programme; Renewable energy obligation; Renewable energy sources

Nomenclature

Abbreviations

CDF	Cumulative density function
DED	Dynamic economic dispatch
DEED	Dynamic economic emission dispatch
DLC	Direct load control
DRP	Demand response programme
DR	Demand response
DSM	Demand side management
DSO	Distribution system operator
EDRP	Emergency demand response programme
EE	Energy efficiency
GSF	Generator shift factor

HEMS	Home energy management system
IPP	Independent power producer
PDF	Probability density function
PV	Photovoltaic
RES	Renewable energy sources
RLM	Residential load management
RO	Renewable obligation
RTP	Real time price
SO	System operator
SR	Spinning reserves
TC	Total cost
TOU	Time of use

Indices and Sets

b	Index of buses
g	Index of thermal generators
l	Index of transmission lines
m	Index of wind generators
N_G	Set of thermal generators
N_L	Set of transmission lines
N_M	Set of wind generators
N_V	Set of photovoltaic generators
N_B	Set of buses
N_R	Set of generator spinning reserves
r	Index of generator spinning reserves
T	Time interval period
v	Index of photovoltaic generators
i	Index of Pareto set

Parameters

α	Renewable energy obligation requirement
γ	Renewable energy penalty cost in US dollars
ρ	Spinning reserve cost coefficient of the gth thermal generator in \$/MWh
τ	PV generator cost in \$/MWh
$\tilde{P}_{b,t}$	System demand after RLM at bus b, and time t in MW
ζ	Wind generator cost in \$/MWh
C_g	Thermal generator g marginal cost
C_m	Wind generator m tariff cost
C_r	Thermal generator spinning reserve r operating cost
C_v	PV generator v tariff cost
DR_g	Ramp down limit for the gth thermal generator in MW/h
$P_{b,t}$	System demand before RLM at bus b, and time t in MW
$P_{g,max}$	Maximum output power from the gth thermal generator in MW
$P_{g,min}$	Minimum output power from the gth thermal generator in MW
$P_{l,t}$	Transmission line power flow at time t in MW
$SRR_{r,max}$	Maximum spinning reserve requirement for the gth thermal generator in MW
UR_g	Ramp up limit for the gth thermal generator in MW/h
$\Delta P_{b,t}$	Demand reduction due to RLM at bus b, and time t in MW
ε	ε -constraint used to change multi-objective optimisation problem into single objective problem

λ_t^R	Real time price of electricity at time t in \$/MWh
$\xi_{b,t}$	Customer willingness to buy electricity at time t in \$/MWh
a_g, b_g, c_g	Thermal generator g cost coefficients
$D_{l,b}$	Generator shift factor for demand at each bus b
$F_{l,m}$	Generator shift factor for wind generators
$G_{l,g}$	Generator shift factor for thermal generators
$H_{l,v}$	Generator shift factor for PVs
$P_{l,max}$	Maximum transmission line thermal capacity in MW
$P_{l,min}$	Minimum transmission line thermal capacity in MW
$P_{m,t,max}$	Achieved wind generation at time t in MW
$P_{v,t,max}$	Achieved PV generation at time t in MW
$SSRR$	System spinning reserve requirement in MW

Variables

$P_{g,t}$	Scheduled output power for thermal generator g at time t
$P_{m,t}$	Scheduled output power for wind farm m at time t
$P_{r,t}$	Scheduled output power for thermal generator spinning reserve r at time t
$P_{v,t}$	Scheduled output power for PV generator v at time t
$u_{b,t}$	A binary variable representing the RLM switching status at bus b , time t

1. Introduction

In recent years there has been a lot of attention on the optimal demand and supply side strategy of energy. From the supply side, the focus has been on reducing conventional generators by increasing the penetration level of renewable energy sources (RES). While on the demand side, several programmes have been introduced to create customer awareness of utilising energy in an efficient manner. The intermittency and stochastic nature of RES such as wind and photovoltaic generators makes it difficult for their integration in the power system. This means that the RES generators cannot be completely regulated by producers throughout the day as they are weather dependent and an increase of RES in power systems requires a robust system. Moreover, the need for capacity margins during peak hour demand coupled with the inherent limited ramping capacity of thermal generators affect the system security and reliability whenever the RES generators decrease their output power due to meteorological conditions. To tackle this challenge, the system operator (SO) takes the advantage of demand side strategy by either shifting or cutting down the load to balance the RES production. Therefore, it is essential to evaluate the effectiveness of demand response (DR) strategy in relation to increasing RES penetration without affecting the system reliability and security.

1.1. Literature review

Demand side management (DSM) has two fields that focus on demand management, i.e., energy efficiency (EE) and demand response programmes (DRP). EE concentrates on retrofitting electrical equipment with more energy efficient equipment while DRP focuses on demand management through price-based or incentive-based demand reduction programmes. Both programmes are used to encourage the customers to use electricity prudently. A comparison between EE and DRP shows that DRP is more cost-effective in terms of capital expenditure, and as a result it is the most common demand management strategy utilised [1,2]. DRP takes advantage of load flexibility patterns to

increase the efficient operation of power system. For example, flexible load from residential customers such as electric water heaters can be shifted to low demand period which improves the system performance and allows the SO to schedule an optimal energy mix at a least operating cost. Flexible demand is, therefore, defined as the potential to modify the consumption profile by varying power consumption, time of operation and the activation time of electrical equipment [3].

DR has two components, i.e., tariff and incentive-based instruments that are used to encourage electricity end-users to respond either to changes in electricity prices over time or provide an incentive to customers for reducing their electricity use. The main idea behind all price-based DR is to encourage electricity end-users to take the advantage of the electricity prices by moving their flexible loads to low demand periods. The types of price-based DR are (i) time-of-use (TOU) pricing, (ii) critical peak pricing, (iii) peak load pricing; and (iv) real-time pricing (RTP) [4].

On the contrary, the incentive-based DR offers customers incentives in addition to their retail electricity rate for achieving demand reduction on the flexible loads when the system reliability is required or when electricity prices are too high. The types of incentive-based DR are (i) direct load control (DLC), (ii) interruptible service, (iii) demand bidding/buy back, (iv) emergency demand response programme (EDRP), (v) capacity market programme; and (vi) various ancillary service markets [5]. The DR is applied to all customers and it is normally implemented on non-critical loads that are reducible and deferrable.

A significant amount of research has been conducted in the combined field of dynamic economic dispatch (DED) and DRP which focuses on different types of customers, e.g., residential, commercial and industrial [6,7]. A day ahead stochastic economic dispatch with price-based DR is implemented in Ref. [8] where maximum wind energy is added into the grid by encouraging the customer to shift their demand profile which improves the utilisation of the wind energy and reduces the total operating cost. The main disadvantage with this type of price based DRP is the direct dependence of the customer behaviour to voluntarily decrease the demand. Moreover, it does not show the impact of direct or indirect load rebound effects ([9,10]) due to the DRP implementation. A more robust approach that provides the system operator (SO) with more control and predictability of the demand is the incentive-based DR. In the US alone, it is estimated that an incentive based DRP can realise up to 93% of the peak load reduction [11]. This direct approach of controlling the customer demand by incentives has resulted in a great deal of interest in researchers. In Ref. [12,13], a stochastic unit commitment with incentive based DRP is presented and a price quantity package for incentive based DRP is reported in Ref. [14]. Authors in Ref. [15] consider a robust optimisation approach to economic dispatch with renewable energy sources and incentive DRP. A DR approach which considers EDRP and DLC based price elasticity and linear responsive loads, i.e., power, exponential and logarithmic models, are presented in Ref. [16]. A combined DED and DR is used to determine an optimal incentive for customers considering different responsive loads.

In [17], a deep neural network for incentive based DRP is reported where the uncertainties in price and demand are studied by deep learning and neural network. This is to ensure that an optimal incentive price is achieved for the energy demand balance and to improve the grid reliability. A combined dynamic economic emission dispatch (DEED) and DRP for industrial customers is presented in Refs. [18] where a game theory demand-based response programme is used to find an optimal hourly incentive that can be offered to customers participated in load curtailment. The model presented in Ref. [19] finds an optimal incentive for customers in order to provide maximum relief to the power system by providing customers incentives for participation throughout the day.

Ref. [20] presents the impact of applying both price-based and incentive-based DR on demand-price elasticity concept while incorporating the customer benefit. In the study, the demand is categorised as flexible load in a micro-grid with residential and commercial customers and the impact of different price and incentive-based schemes are investigated. In Ref. [21], a DR scheduling model is presented for smart residential community. The residential loads are classified into different categories based on

their demand response capability, i.e., interruptible load, controllable loads and deferrable loads, and thereafter, the load is reduced from peak to peak-valley without bringing any customer discomfort. The integration of distributed generators (DG) is also included to better manage the demand shifting. This study does not incorporate the load rebound effects which results from deferrable load shifting from peak demand period to low demand period. In South Africa, the main electricity supplier has developed a large-scale residential load management (RLM) programme which is aimed specifically at the residential sector [22]. The electric water heaters, also known as geysers, account for about 30% and 50% of the electricity consumption in a household [23] and the load can be classified as deferrable. Moreover, the utility's residential customers consume around 20%–25% of the total electricity generated with their peak period amounting to 35%. The RLM programme involves the connection of ripple control units to electric water heaters which allows the units to be switched on and off remotely by the SO.

Although all the studies have focused on providing a combined benefit from demand and supply side, the disadvantages with their proposed methods are: (i) the level of customer discomfort caused by regular demand reduction, (ii) the inability of the theoretical DRP models to include the load rebound effects that result from demand reduction programmes due to arbitrary control of flexible load. The literature review shows that residential flexible loads under DR with DLC is performed during periods of high electricity cost and in Ref. [24] the authors do not show the impact of load increase outside of the peak period and this implies that the flexible load is reducible. Reference [25] did not quantify the demand reduction due to deferrable loads in their models. In cases where storage is used [26,27] the authors assume that the cost of electricity from storage is lower than the utility low tariff price which implies that the flexible load during peak hours is automatically supplied by the storage system. Although this may be a benefit, it is important to note that there are cases where the cost of storage is higher than that of the utility and this is not shown in the literature [28,29]. The use of DG and RES to offset the electricity prices is also proposed by other authors [30,31]. This approach is generally acceptable since the flexible load can be supplied by RES or DG, however, there is also a challenge with this approach since RES is intermittent and may not be available during peak period or the generation may be inadequate to supply the demand. Lastly, most DRP with flexible residential loads in the literature assume that the deferrable loads do not have load rebound effects and this is mainly due to the lack of real data.

1.2. Research objectives

To address these challenges, this paper aims to develop a combined demand and supply side economic dispatch model. This includes the RO policy framework to maximise RES penetration and deferring residential flexible demands to period of low electricity price. The renewable obligation (RO) policy aims to ensure that the deferrable demand can be supplied from RES during peak hours by ensuring that a quota of RES generation is achieved. The customer discomfort level is minimised by limiting the demand reduction to electric water heaters. All participating residential customers have a smart home energy management system (HEMS) which incorporates a DLC unit connected to the electric water heaters that allows remote switching. The main contributions of this paper are summarized as follows:

1. A multi-objective economic dispatch model is presented which integrates deferrable demand within a real DLC DRP intermittent renewable energy under RO framework;
2. Real data from a South African DRP are taken in the optimisation model so that the SO can decide whether a substation needs to respond to the DR request;
3. The application of the real DRP data avoids traditional inaccurate approaches in assuming the arbitrary controllability of deferrable load and can cover actual load rebound effect.

1.3. Paper organisation

The contents of this paper are organised into six sections. In Section 2, the RLM framework is developed. In Section 3, the mathematical model for the RO, RLM and RES are developed and in Section 4, the method for handling multi-objective optimisation is presented. In Section 5, the feasibility and efficiency of the proposed model are investigated on two test systems. Finally, in Section 6, the conclusions are drawn.

2. Residential load management framework

RLM is a utility programme that is focused on residential customers with the objective of reducing and shifting the customers flexible load during peak demand periods. The flexible load considered in the programme is the electric water heater.

The residential customers are generally connected at the end of the power grid, while large-scale wind and PV plants are normally connected to the transmission power network as shown in Fig. 1.

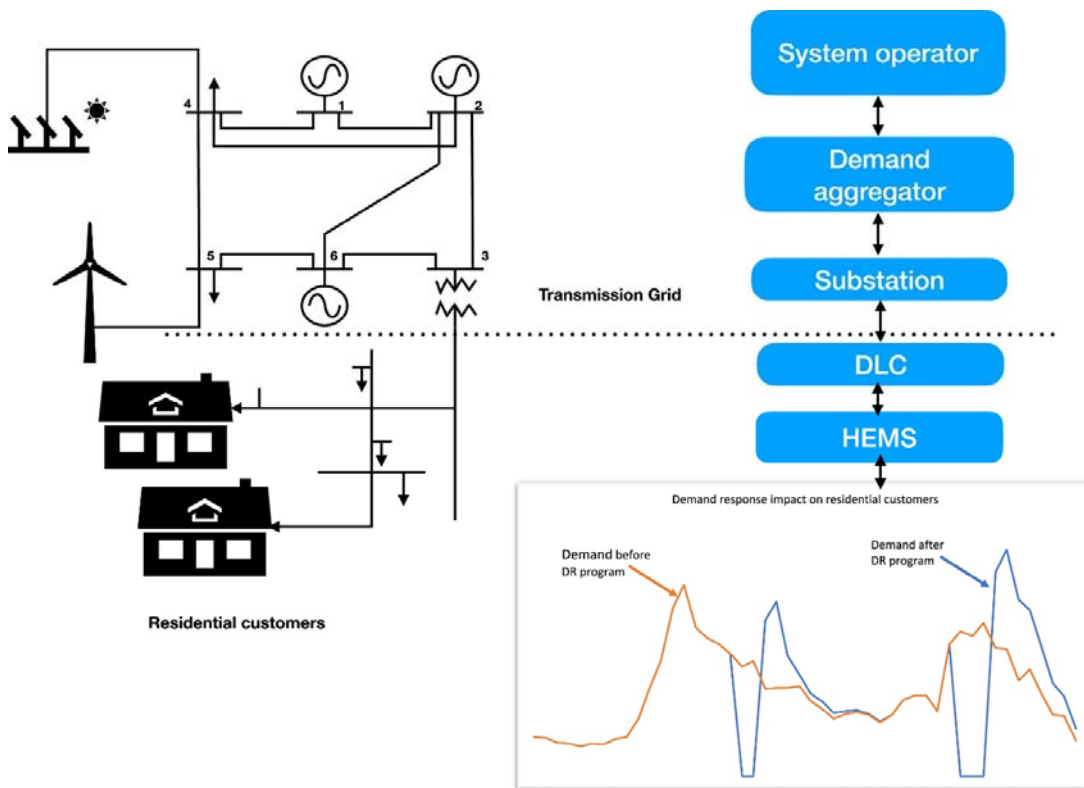


Fig. 1. Typical RLM programme structure based on an arbitrary 6 bus network.

On the residential demand side, all the customers participating in the DRP use a DLC unit which is integrated to the two-way smart metering system to send real-time status of the electric water heater. The customers are aggregated together on each participating substation. A municipality distribution system operator (DSO) acts as a demand aggregator and facilitates the communication between the SO and the customers. The real-time data are used by the utility to manage real-time demand on the power system. In the RLM programme implemented in South Africa, the residential customers participate on a voluntarily basis. However, in this proposed model an incentive is paid to participating customers. In fact, the SO uses DRP as a tool for load shifting and pays an incentive proportional to demand reduction achieved. The customers can choose to participate in the

programme during peak demand periods where electricity price is high. If the consumers chose to participate in the programme the demand is reduced and deferred to low demand period and the customers receive an incentive. On the contrary, if the customer declines to participate then the customer pays high electricity price associated with peak demand. All the real-time demand information is managed through a HEMS.

The utility owns all the thermal generators while the RES is owned by independent power producers (IPPs). The SO is responsible for controlling and dispatching all generators to meet the demand and achieve RO. The DSO is responsible for managing the residential participation to the DRP programme through the substation DLC system. The demand is modelled like negative generation with the minimum and maximum load changes based on customer participation level [32]. The main objective from the SO point of view is to dispatch all the generators to meet the demand while minimising the cost for thermal generators and achieving a RO with minimum power fluctuations from RES generators by utilising DR.

3. Problem formulation

In this section a mathematical model of the RO policy framework which incorporates the DRP for residential customers is presented. In Section 3.1 the RO model is presented and then followed by the RLM model in Section 3.2. Finally, the model of RES is presented in Section 3.3.

3.1. Renewable obligation framework

The main purpose here is to minimise the total operating cost for the system operator thermal generators while maintaining a percentage of renewable energy in the energy mix. The renewable obligation model is extended from Ref. [33,34].

3.1.1. Objective functions

The total operating cost includes two terms. The first term is the cost of operating thermal generators and the cost paid to IPP for RES generators. The second part is the penalty function that ensures that a minimum renewable obligation is maintained in the dispatch period to guarantee the required energy mix.

$$\phi_1 = \sum_{t=1}^T \left(\sum_{g=1}^{N_G} C_g (P_{g,t}) + \sum_{r=1}^{N_R} C_r (P_{r,t}) + \sum_{m=1}^{N_M} C_m (P_{m,t}) + \sum_{v=1}^{N_V} C_v (P_{v,t}) \right) + \mathcal{I} \quad (1)$$

Where $C_g (P_{g,t})$ is the generator fuel cost function which is a quadratic equation, and $C_r (P_{r,t})$ is the spinning reserve operating cost and $C_m (P_{m,t})$ and $C_v (P_{v,t})$ are the cost function for wind and PV generators, respectively, as shown in (2) to (5).

$$C_g (P_{g,t}) = \sum_{g=1}^{N_G} \left(a_g P_{g,t}^2 \Delta t^2 + b_g P_{g,t} \Delta t + c_g \right) \quad (2)$$

$$C_r (P_{r,t}) = \sum_{r=1}^{N_R} \rho_r P_{r,t} \Delta t \quad (3)$$

$$C_m (P_{m,t}) = \sum_{m=1}^{N_M} \zeta_m P_{m,t} \Delta t \quad (4)$$

$$C_v (P_{v,t}) = \sum_{v=1}^{N_V} \tau_v P_{v,t} \Delta t \quad (5)$$

Note that in this paper $\Delta t = 1$ which means that the sampling period is 1 h. The notation \mathcal{Y} is the second part of the total cost which is the renewable obligation part of the model shown in (6).

$$\mathcal{Y} = \gamma \sum_{t=1}^T \left(\alpha \left(\sum_{g=1}^{N_G} P_{g,t} + \sum_{m=1}^{N_M} P_{m,t} + \sum_{v=1}^{N_V} P_{v,t} \right) - \left(\sum_{m=1}^{N_M} P_{m,t} + \sum_{v=1}^{N_V} P_{v,t} \right) \right)^+ \quad (6)$$

where γ is the penalty imposed to the thermal generators for not achieving the renewable obligation, α is the renewable obligation requirement in percentage. The sign function $(\cdot)^+$ which is equal to γ if the RES obligation is unattained and 0 otherwise. The penalty γ is normally provided by the energy regulator as an annual value. This penalty value can be changed to a daily penalty value corresponding to daily economical dispatch of generators.

3.1.2. Maximise renewable energy penetration

The second objective function increases the level of RES penetration as presented in Ref. [33]. In addition to the total operating cost in (1), the maximisation of RES penetration is shown in (7).

$$\phi_2 = \sum_{t=1}^T \left(\sum_{m=1}^{N_M} P_{m,t} \Delta t + \sum_{v=1}^{N_V} P_{v,t} \Delta t \right) \quad (7)$$

3.1.3. Constraints

Constraint (8) means that the total power generated from wind, PV and thermal generators is equal to the demand per hour at each load bus. Constraints (9) to (12) show the maximum allowable ramp rate of the thermal generators. Constraints (13) to (16) are the thermal, wind and PV maximum capacities. Constraint (17) means that the sum of the thermal generator and spinning reserve is limited by the generator capacity. While constraint (18) shows that the maximum spinning reserve of each generator cannot exceed the thermal generator capacity. Constraint (19), ensures that the spinning reserve over a dispatch period is greater than the system spinning reserve requirements. Constraint (20) ensures that there is adequate spinning reserve to ensure that the demand can be covered by the thermal generators if the RES generators are not available to produce any power. Constraints (21) and (22) represent the transmission flow limits which are estimated using DC power flow.

$$\sum_{g=1}^{N_G} P_{g,t} + \sum_{m=1}^{N_M} P_{m,t} + \sum_{v=1}^{N_V} P_{v,t} = \sum_{b=1}^{N_B} P_{b,t} \quad \forall t \quad (8)$$

$$P_{g,t} - P_{g,t-1} \leq UR_g \Delta t \quad \forall t, \forall g \quad (9)$$

$$P_{g,t-1} - P_{g,t} \leq DR_g \Delta t \quad \forall t, \forall g \quad (10)$$

$$P_{r,t} - P_{r,t-1} \leq UR_r \Delta t \quad \forall t, \forall r \quad (11)$$

$$P_{r,t-1} - P_{r,t} \leq DR_r \Delta t \quad \forall t, \forall r \quad (12)$$

$$P_{g,t} \leq \min(P_{g,max}, P_{g,t-1} + UR_g \Delta t) \quad \forall t \quad (13)$$

$$P_{g,t} \geq \max(P_{g,min}, P_{g,t-1} - DR_g \Delta t) \quad \forall t \quad (14)$$

$$P_{m,t} \leq P_{m,t,max} \quad \forall t \quad (15)$$

$$P_{v,t} \leq P_{v,t,max} \quad \forall t \quad (16)$$

$$P_{g,t} + P_{r,t} \leq P_{g,max} \quad \forall t, \forall g \quad (17)$$

$$0 \leq P_{r,t} \leq SRR_{r,max} \quad \forall t \quad (18)$$

$$\sum_{r=1}^{N_R} P_{r,t} \geq SSRR \quad \forall t \quad (19)$$

$$\sum_{g=1}^{N_G} P_{g,t} + \sum_{r=1}^{N_R} P_{r,t} \geq \sum_{b=1}^{N_B} P_{b,t} \quad \forall t \quad (20)$$

$$-P_{l,max} \leq P_{l,t} \leq P_{l,max}, \quad \forall t, \forall l \quad (21)$$

$$P_{l,t} = \sum_{g=1}^{N_G} G_{l,g} P_{g,t} + \sum_{m=1}^{N_M} F_{l,m} P_{m,t} + \sum_{v=1}^{N_V} H_{l,v} P_{v,t} - \sum_{b=1}^{N_B} D_{l,b} P_{b,t} \quad (22)$$

The maximum spinning reserve requirement $SRR_{r,max}$ is equal to the maximum thermal generator capacity, and the system spinning reserve requirement (SSRR) is equal to 30% of demand $P_{b,t}$; where $G_{l,g}$, $F_{l,m}$, $H_{l,v}$, and $D_{l,b}$ denote the generator shift factor (GSF) coefficient between line l and thermal generator, wind farms, PV plant, and system demand at each bus. The transmission line power $P_{l,t}$ of line l at time interval t is calculated using DC power flow.

3.2. Residential load management

The programme considers voluntary participation by residential customers to reduce and shift their demand. However, in this case the DRP model assumes an incentive is paid to participating customers. The load reduction request from the utility can be anytime of the day and particularly when the demand is high.

3.2.1. Demand response programme model

The price-based DR objective function presented in (23) is known as the customer utility function which aims to minimise the discomfort level due to the lack of electricity.

$$\begin{aligned} \phi_3 = & \sum_{t=1}^T \sum_{b=1}^{N_B} \left(\left(\lambda_t^R - \xi_{b,t}^c \right) \left(P_{b,t} (1 - u_{b,t}) + \tilde{P}_{b,t} u_{b,t} \right) \right) \Delta t \\ & + \sum_{t=1}^T \sum_{b=1}^{N_B} \Delta P_{b,t} u_{b,t} \xi_{b,t}^i \end{aligned} \quad (23)$$

Equation (23) refers to the total cost associated with minimising the customer discomfort level which measures the benefit the consumer achieves by using electricity during time period t , λ_t^R is the TOU price of electricity while $\xi_{b,t}^c$ is the benefit or willingness of the customer to buy electricity for performing tasks requiring electricity. For simplicity, the benefit for the consumer is assumed to be constant and time independent, which implies that the residential load is deferrable since the task can be performed at any time during the day [35].

To encourage residential customer participation, an incentive is introduced to the model to quantify the impact of demand reduction and demand deferred as a result of the incentive the residential customers are incentivized only during peak hours which is assumed to correspond to high demand period.

The incentive price paid to customers is $\xi_{b,t}^i$ and $\Delta P_{b,t}$ is the difference between the actual demand at the participating DRP bus b before and after the demand reduction.

$$\Delta P_{b,t} = P_{b,t} - \tilde{P}_{b,t} \quad (24)$$

The DLC switching status $u_{b,t}$ is a binary variable that is equal to 1 if the RLM is implemented at bus b in time t and 0 indicating that no RLM is implemented.

3.2.2. Constraints changes

The only changes in the constraints are due to the change in demand which is replaced by (25); the constraints affected by the demand reduction are (8), (19), and (20). The change of constraint (19) is due to the fact that SSRR is equal to 30% of demand $P_{b,t}$ to guarantee enough spinning reserves.

$$P_{b,t} = \sum_{b=1}^{N_B} \left(P_{b,t} (1 - u_{b,t}) + \tilde{P}_{b,t} u_{b,t} \right) \quad \forall t. \quad (25)$$

The two cost functions can be added together to form a new objective function as shown in (26).

$$\phi_{TC} = \phi_1 + \phi_3 \quad (26)$$

3.3. Modelling of renewable energy sources

In this section a statistical modelling of wind and PV generators is presented using unimodal and bimodal Weibull probability density function (PDF).

The wind energy system is modelled using a unimodal Weibull PDF and the PV generator is modelled using bimodal Weibull PDF as presented in Refs. [33]. The statistical modelling techniques used for PV and wind generators can be found in Ref. [[36], [37], [38]].

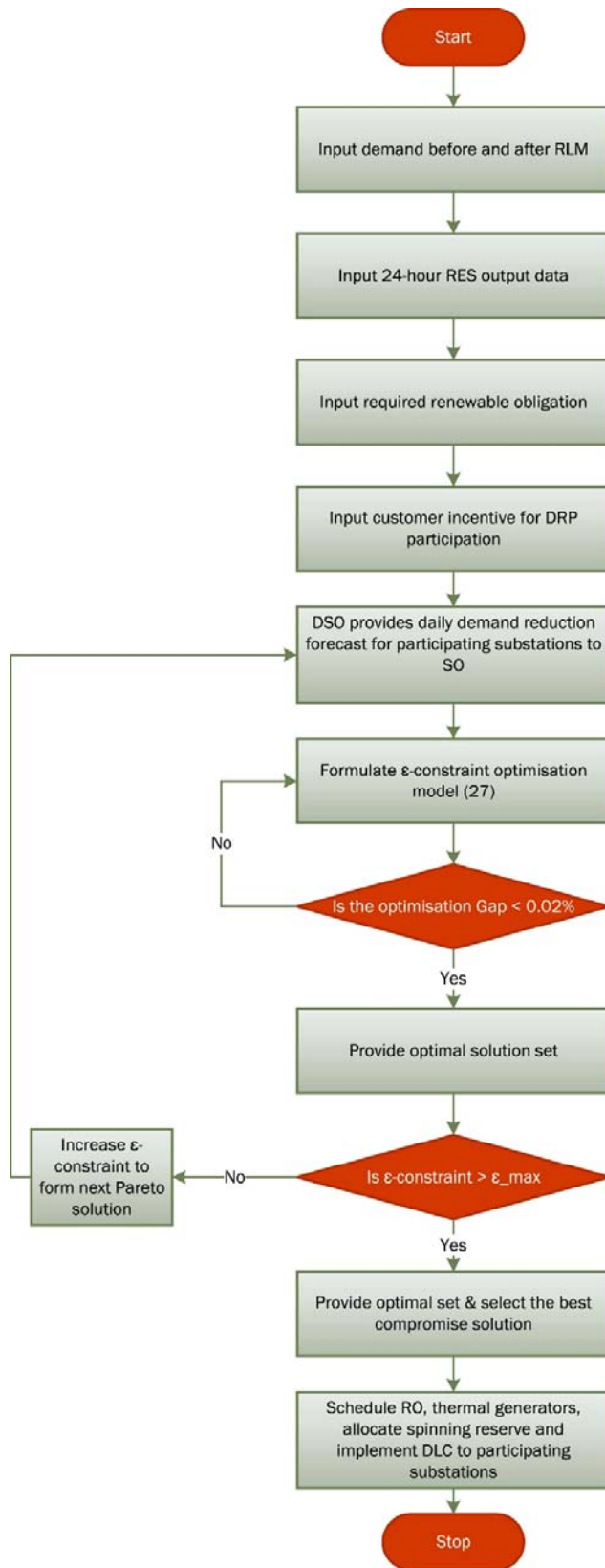


Fig. 2. A step-by-step approach to estimating wind and PV PDF parameters and output power.

3.3.1. Implementation steps for RES selection and output power estimation

The step-by-step approach for selecting RES location and estimate RES output are as follows

1. Collect 1-year data for wind speed [39] and solar irradiance [40] related to each wind and PV site.
2. Pre-data processing: remove measurement errors and outliers.
3. Formulate a histogram of the wind speed and solar irradiance data.
4. Calculate the average wind and solar power density from the real data.
5. Fit the histogram with the best PDF or multi-modal PDF, i.e., Weibull and bimodal Weibull.
6. Estimate the initial parameters of the PDFs.
7. Calculate the wind and solar power density of the histogram which also includes the PDF.
8. Calculate the sum of wind power density and solar power density.
9. Estimate the PDF parameters using least square method in excel solver by finding the best parameters that match the wind and PV power density curves [33].
10. Calculate the wind and solar cumulative density function (CDF) functions based on the estimated parameters.
11. Forecast wind power and PV output power

A flow chart representing a step-by-step approach is shown in Fig. 2.

4. Multi-objective optimisation approach

There are generally several approaches that can be utilised to solve a multi-objective problem in the literature. These methods are typically, the weighted sum [41], global criterion [42] and ε -constraint [43] to mention a few. In this paper, ε -constraint method is used to change the multi-objective optimisation problem into a single objective problem. The reason for selecting this method originates from the fact that it is efficient for solving non-convex and non-linear problems such as the one presented. A single objective function is considered in the ε -constraint methods while the other objectives are changed into constraints as shown in (27).

$$\begin{aligned} \min \quad & \phi_{TC} \\ \text{s. t.} \quad & \sum_{m=1}^{N_M} P_{m,t} \Delta t + \sum_{v=1}^{N_V} P_{v,t} \Delta t \geq \varepsilon_i \quad \forall t, \forall i \end{aligned} \quad (27)$$

(8)–(22)

Where ε_i is the Pareto solution set in $i \in (0,10)$, that is increased from the minimum to the maximum value to generate a Pareto front. The minimum and maximum values of the constrained objective function are calculated by maximising and minimising those functions. Thereafter, the ε -constraint bounds increase from the minimum to the maximum function. In this paper, a preference-based approach similar to Ref. [41] is used for the best compromise solution in a Pareto optimal set.

5. Numerical case studies

The modified IEEE 30-bus and IEEE 118-bus test systems are used to validate the proposed DRP model over a 24-h time horizon using a temporal resolution of 60-min. The historical data of RES generators is collected over a period of a year from January 1st, 2018 to December 31st, 2018 and it can be found in Ref. [39,40]. The system load is obtained from a real RLM study performed in SA [44] which also includes the total number of electric water heaters used, the capacity and the temperature range of the storage tank. The modified IEEE 30-bus system has 6 thermal units and 41

transmission lines. The system data for IEEE 30-bus can be found in Ref. [45], which includes all the ramp rates, thermal transmission limits and quadratic cost coefficients for the thermal units.

The modified IEEE 118-bus system consists of 54 thermal generators and 186 transmission lines. The system detailed data of units and network parameters can be found in Ref. [46]. A total of 10 RES generators (5 PV and 5 wind farms) are added to the network on buses 1, 33, 38, 52, 58, 75, 96, 102 and 117. The transmission line flow limit is simulated using DC power flow at a sampling interval of 60-min. In all the simulation studies, a RES penetration level of 10% is used as a benchmark. In the case where RES penetration level is not achieved a penalty of \$100,000 per day is imposed. In addition, the system spinning reserve required is based on 30% of the maximum demand and the spinning reserve of each generator is equal to the maximum generator capacity.

The DSO is responsible for implementing the RLM switching at the substation based on SO DRP requirement. An incentive of \$40 per MWh is paid to participating customers for achieving demand reduction. The utility sell electricity to all customers based on the TOU and RTP. The electricity price for peak, off-peak and standard period is \$200/MWh, \$50/MWh and \$100/MWh respectively. The customer willingness to buy electricity is \$120/MWh and \$50/MWh for TOU and RTP respectively. In this study, peak period is classified as 07:00 to 09:00 in the morning, 18:00 to 20:00 in the evening; the standard period is from 09:00 to 18:00 and from 20:00 to 21:00 and remaining period is classified as off-peak. Moreover, the participating customers can only receive an incentive during peak period.

The simulation is conducted on a notebook with an Intel Core i5 at 2.70 GHz and 8 GB of RAM. The optimisation model is a mixed integer quadratic programming (MIQP) problem and it is built in IBM ILOG CPLEX. The tolerance gap in the CPLEX solver is set to 0.02%. To show the effectiveness of the DRP RO model, the effects of operating cost, spinning reserve allocation, incentive cost, substation participation to RLM programme, RES penetration increase, peak RES increase or decrease, peak demand reduction, demand deferred to other time periods and total demand reduction are analysed. The DRP RO model is tested on the modified IEEE 30-bus system considering the following cases.

1. A base case scenario which considers the proposed model without the implementation of DRP;
2. The implementation of the proposed model with DRP DLC considering TOU tariff;
3. The implementation of RTP of electricity on the proposed model; and
4. A comparison of the base case to the proposed DRP DLC model.

Thereafter, IEEE 118-bus system is also used to test the model on a large scale and the sensitivity of the model to RES penetration against DRP DLC in terms of spinning reserve, total demand reduction and increase in RES penetration.

5.1. Implementation steps

The step-by-step approach for implementing the DRP RO model for a combined energy and reserve dispatch is as follows.

1. Input demand before and after RLM, 24-h RES output data, TOU tariff, incentive cost for DRP participation and customer willingness cost of electricity.
2. DSO provides daily demand reduction forecast for participating substations to SO.
3. Formulate ϵ -constraint optimisation model.
4. Evaluate RO and DRP requirements.
5. Provide an optimal Pareto set.
6. Implement preference-based approach to select the best compromise solution using lower and upper boundaries provided by the SO.
7. Schedule RO and DLC to participating substations according to the best compromise solution.

The overall implementation flow chart is shown in Fig. 3.

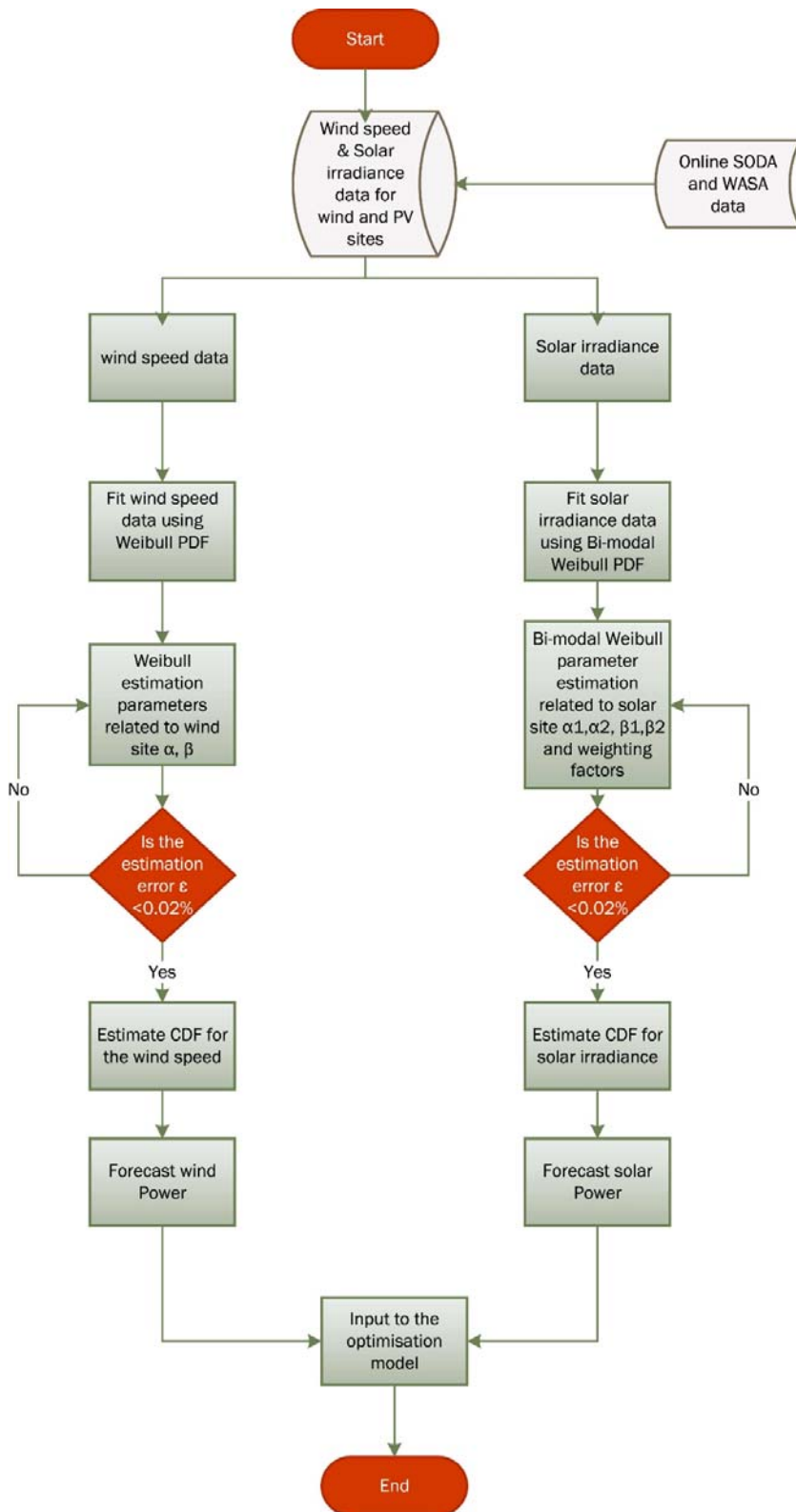


Fig. 3. Optimisation algorithm for solving multi-objective DRP-RO model with Pareto optimal set and preference-based approach for selecting the best compromise solution.

5.2. Modified IEEE 30-bus

The modified IEEE 30-bus test system has a total demand before and after RLM of 26822.5 MW and 26501.3 MW. The integrated PV and wind farms are connected to buses 7, 15, 22, and 24, i.e., two PV plants and two wind farms. The sizes of the PV and wind farms are 75 MW, 140 MW, 300 MW and 500 MW with an installed capacity of 1015 MW. The parameters of thermal units and RES generators are listed in Table 1, Table 2, Table 3 respectively [33].

Table 1. Thermal generator parameters.

Unit	Pmin	Pmax	a_g	b_g	c_g	RU	DR
G1	50	350	0.0070	7	240	60	60
G2	50	250	0.0095	10	200	60	60
G3	50	150	0.0090	8	220	60	60
G4	50	350	0.0090	11	200	60	60
G5	50	450	0.0080	10.5	220	60	60
G6	50	500	0.0075	12	190	60	60

Table 2. PV solar irradiance profile for site 1 and 2.

Description	PV 1	PV 2
$K_c (W/m^2)$	150	150
$\Omega (W/m^2)$	1000	1000
B	0.5	0.600
κ_1	0.8	1.2
κ_2	4.13	5.4
$\sigma_1 (W/m^2)$	150	140
$\sigma_2 (W/m^2)$	900	980

Table 3. Wind speed profile for site 1 and 2.

Description	Wind 1	Wind 2
K	1.70	2.0
$\sigma (m/s)$	6.653	5.0

The RLM programme is applied to load buses, also referred to as substations. The substations participating in the RLM programme are located on buses 10, 14, 23 and 26. The total demand before and after the implementation as well as the forecasted RES penetration is shown in Fig. 4 and the electricity price is shown in Fig. 5.

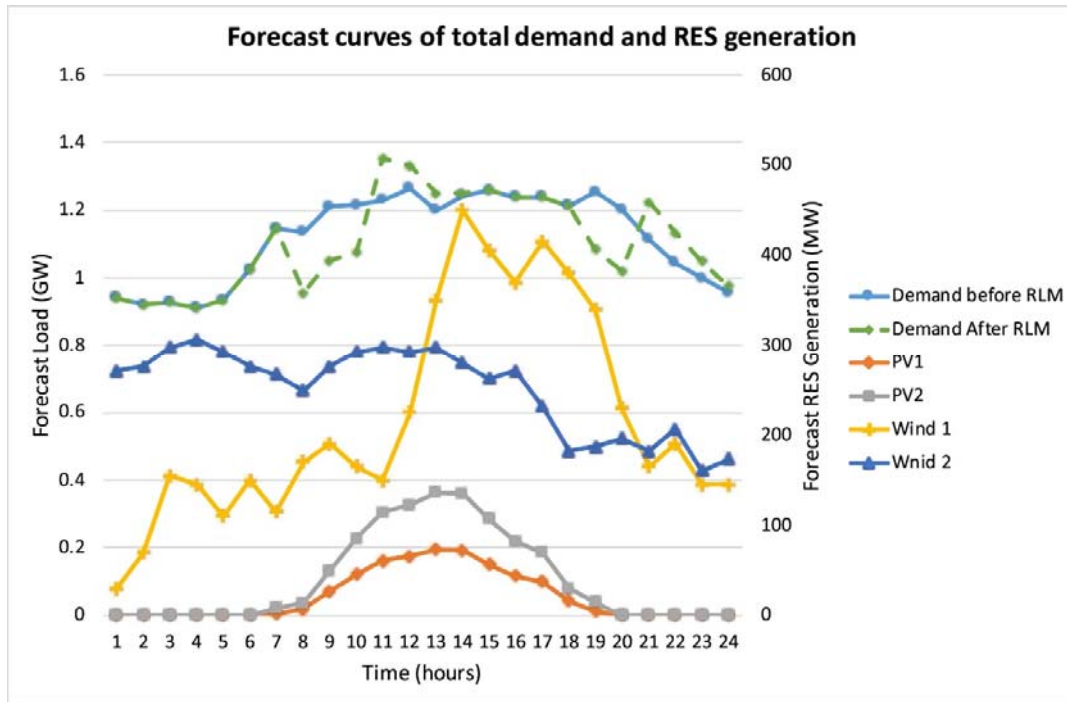


Fig. 4. Forecasted demand and RES generation before RLM is implemented.

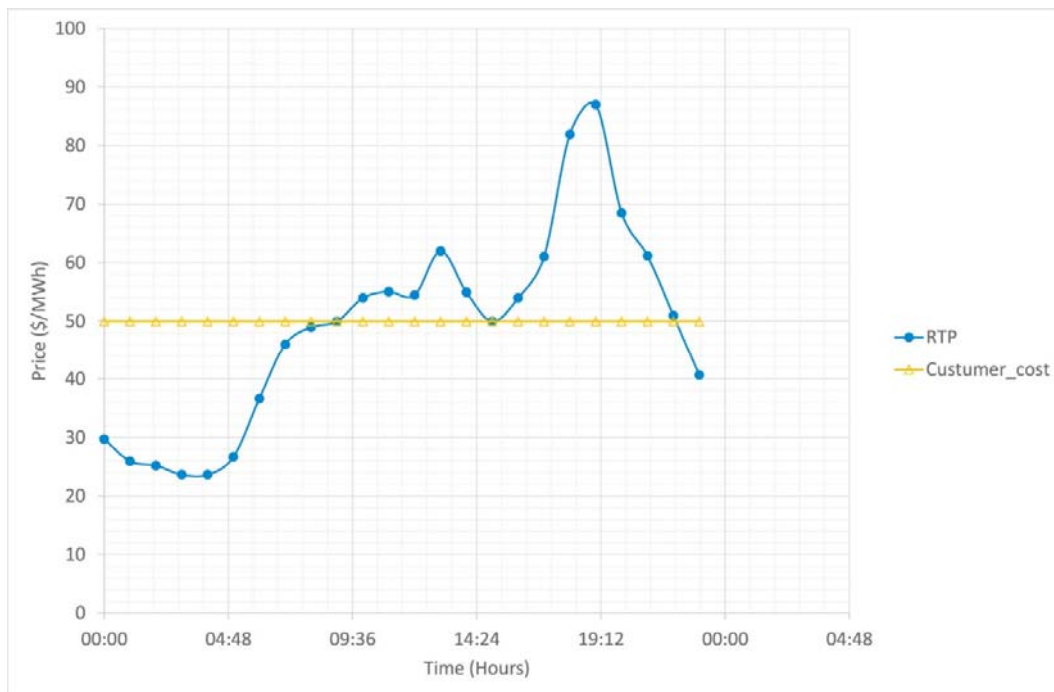


Fig. 5. Real time price of electricity and the customer price of electricity.

5.2.1. Normal operation without demand response

In this case the normal operation without DR is investigated in terms of total operating cost, maximum achieved RES penetration and the allocated spinning reserves. In the first case, a Pareto front is used to select the best compromise solution for the multi-objective optimisation problem. The minimum and maximum values of the two objective functions are calculated and thereafter, the ϵ -constraint method is used to generate multiple solutions related to the changes of the ϵ -constraint. Table 4 shows the Pareto optimal set for different RES penetration level.

Table 4. Pareto optimal set under renewable obligation of 10%.

Pareto	RES (MWh)	TC (\$)	SR (MW)
<i>0</i>	<i>7934.70</i>	<i>313,870.00</i>	<i>8168.1</i>
1	7983.70	313,880.00	8215.90
2	8053.70	313,890.00	8283.00
3	8115.30	313,910.00	8341.00
4	8149.90	313,930.00	8370.90
5	8158.00	313,940.00	8377.10
6	8159.80	313,945.00	8379.10
7	8160.80	313,950.00	8382.90
8	8172.10	313,980.00	8389.80
9	8241.00	314,520.00	8456.80
<i>10</i>	<i>8592.30</i>	<i>1,102,400.00</i>	<i>30983</i>

The italic values refer, to the minimum and maximum values used in formulating the Pareto set. To select, the best compromise solution from a Pareto optimal set, the SO is the main decision marker. In this case the lower and upper boundaries related to the total operating cost and RES penetration level are set to \$400,000 and 8100 MWh. From the SO boundaries, the best compromise solution is highlighted in bold as depicted in Table 4. A detailed analysis of the best compromise solution for a 24-h dispatch period is shown in Fig. 6.

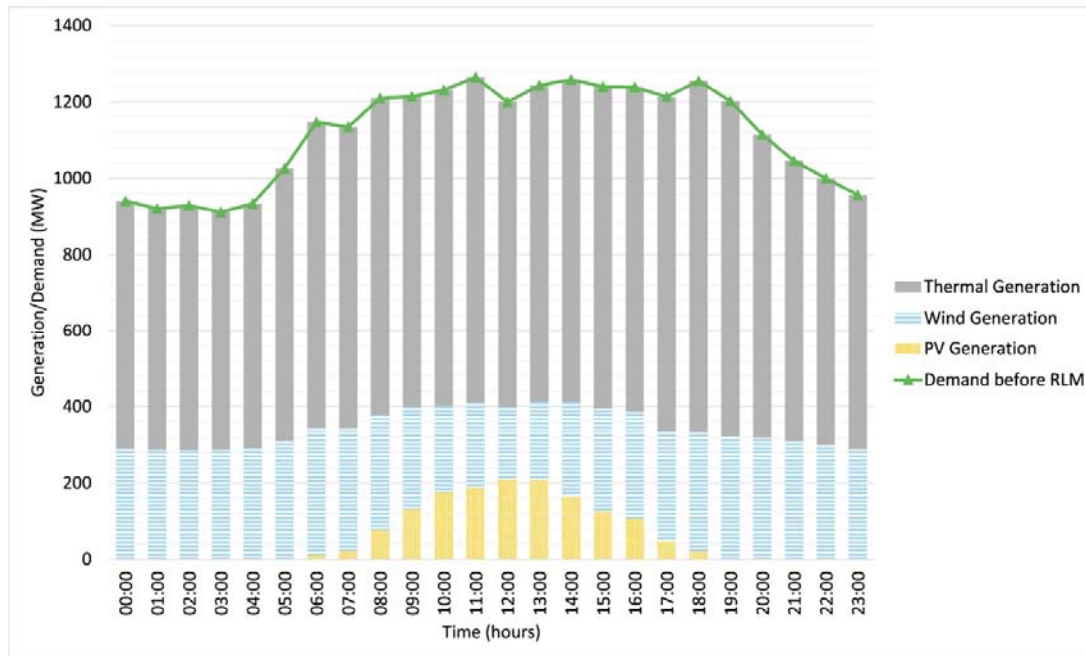


Fig. 6. Demand and generation for 24-h dispatch period considering 10% RES penetration level.

Table 5. Pareto optimal set under renewable obligation of 10% and DLC.

Pareto	RES (MWh)	TC (\$)	SR (MW)
0	7951.30	245,630.00	8080.20
1	7987.60	245,640.00	8116.60
2	8044.00	245,650.00	8173.20
3	8095.20	245,670.00	8224.40
4	8111.20	245,680.00	8240.40
5	8112.20	245,684.00	8241.30
6	8113.60	245,688.00	8242.70
7	8134.50	245,720.00	8263.50
8	8174.60	245,840.00	8303.30
9	8296.30	246,670.00	8424.80
10	8592.30	1,091,700.00	31381.0

The best compromise solution is highlighted in bold and corresponds to RES penetration level of 8296.30 MWh and total operation cost of \$246,670.00.

The generation from thermal units makes up the largest contribution, which is followed by RES generators. The total operation costs for supplying electrical demand is \$314,520. The thermal units generate 18581.5 MWh (69.28%) and RES generators contribute 8241.01 MWh (30.72%) to the total demand. A maximum of 8456.80 MW is allocated for spinning reserve services.

5.2.2. Implementation of incentive based DRP

The demand on the IEEE 30-bus test system is divided into deferrable, firm and reducible loads. The demand before and after the RLM is depicted in Fig. 4. In this case, the impact of DLC is evaluated considering the operation costs, spinning reserve allocation, substation participation level, incentive paid to customers, total RES and thermal generation levels and the achieved demand reduction. A Pareto optimal set is shown in Table 5 as well as the best compromise solution according to the SO.

When DRP is implemented on the substations, the total demand reduced during peak hour period is 830 MW while the demand deferred from peak to valley period and off-peak is 509.72 MW. The difference between the peak demand reduction and deferred load is 321.12 MW which is the actual achieved demand reduction due to DLC implementation. This is properly shown in Fig. 7 where the RES and thermal unit generation makes up the hourly demand.

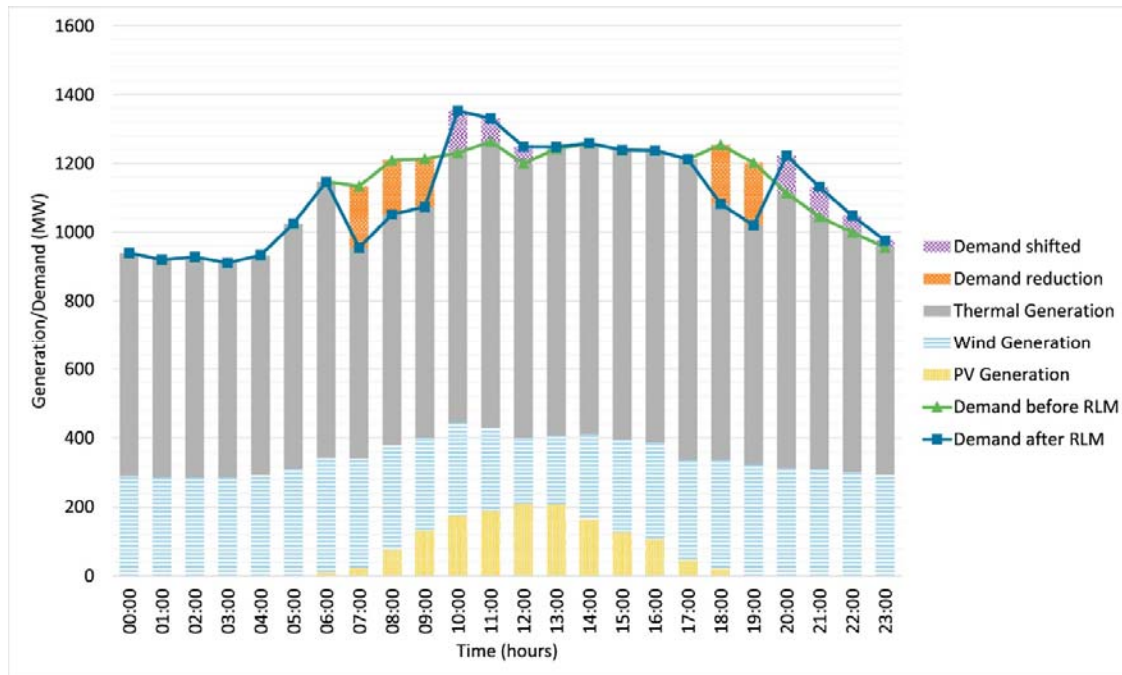


Fig. 7. Demand and generation for a 24-h dispatch period under 10% RES penetration and DLC.

From Fig. 7 the morning peak corresponds to the time when wind power is available, and PV production is low. The total generation from thermal and RES units over a 24-h period is 18205 MWh (68.69%) and 8296.34 (31.31%), respectively, while the spinning reserve allocation is 8424.79 MW. The substations contributing to RLM programme are active during peak hours which means they have reduced their loads. In total, throughout the peak period the RLM substation are actively participating in the programme. This brings in a total incentive of \$12,844.8 to all the customers participating in the RLM.

The reduction in demand during peak-demand period assists in lowering the system stress on the flexible units to supply peak demand and reduce the overall operating costs. Moreover, the increase in

demand in other period contributes to lowering the power production of highly loaded base load generating units.

The selection of renewable obligation as $\alpha = 10\%$ is used as a benchmark for comparison purposes which is a very conservative renewable obligation requirement. This case study shows that the achieved RES penetration is 31.31% which is higher than the required 10%. This implies that for the small-scale IEEE 30-bus network a maximum RES penetration of 31.31% can be achieved without any penalty imposed. This is to say, for any α between 10% and 31.31%, there would not be any penalty imposed. When α is greater than 31.3%, there will be penalty incurred. For example, when $\alpha = 40\%$, the total operating cost is \$356,670 and when $\alpha = 50\%$ the total operating cost is increased to \$476,490.

The achieved demand reduction is also dependent on the renewable obligation requirement. For example, if the RO is increased then the demand reduced will also increase to allow for more RES penetration. However, this increase is limited by the available RES generation and transmission thermal limits. The proposed model shows that a maximum of 31.31% RES penetration can be achieved by reducing 830 MW of demand during peak hours and deferring 321 MW to off-peak hours.

5.2.3. The implementation of RTP of electricity on the proposed model

In this case study the proposed model is tested using RTP of electricity in order to measure the increase in RES penetration and the associated operating costs. The RTP price is different from the TOU price in that the market demand determines the prices of electricity. Fig. 5, shows the RTP price of electricity [47]. Table 6 shows the impact of implemented DRP using RTP for different Pareto set solutions.

Table 6. Pareto optimal set under renewable obligation of 10% using RTP of electricity.

Pareto	RES (MWh)	TC (\$)	SR (MW)
0	7761.30	303,080.00	8291.3
1	7781.40	303,110.00	8291.30
2	7811.10	303,210.00	8291.50
3	7858.10	303,370.00	8291.90
4	7928.40	303,550.00	8292.80
5	7981.00	303,620.00	8294.40
6	8005.00	303,700.00	8297.40
7	8069.00	303,800.00	8303.90
8	8122.00	303,950.00	8315.30
9	8500.70	305,690.00	8630.70
10	8611.20	1,090,600.00	30,989.00

The bold text refers to the selected Pareto optimal solution.

The first and the last Pareto index solutions are the Pareto end points which are also known as anchor points. For example, the first Pareto anchor (0) point is related to a requirement that minimises the operating costs and the last anchor point (10) is related to maximising the RES penetration level. The selected Pareto point (8) shows a RES penetration of 8122 MWh with the operating cost of \$303,950. This point corresponds to a demand reduction of 570 MW and an increase in RES penetration of 1.27% with a total incentive of \$16,617 when compared to a case without DRP.

A comparison of Table 5, Table 6, shows that the maximum energy penetration using TOU is 21.57% compared to 6.14% using RTP. This corresponds to Pareto point (9) of the two tables. The energy penetration is increased when using the RTP compared to when using the TOU tariff. Using the same Pareto point (9), the energy penetration is increased from 0.67% to 0.89%. A comparison between TOU and RTP shows that from a cost savings point of view, TOU has a higher cost savings. However, from a RES penetration point of view, RTP shows better performance. This is only applicable to the IEEE 30 bus test system.

5.2.4. A comparison between base scenario and DRP DLC scenario

In this case study a comparison of Section 5.2.1 and Section 5.2.3 is conducted. In the first case a Pareto front curve for the two scenarios is presented in Fig. 8 which shows the two curves based on whether the DLC is implemented or not.

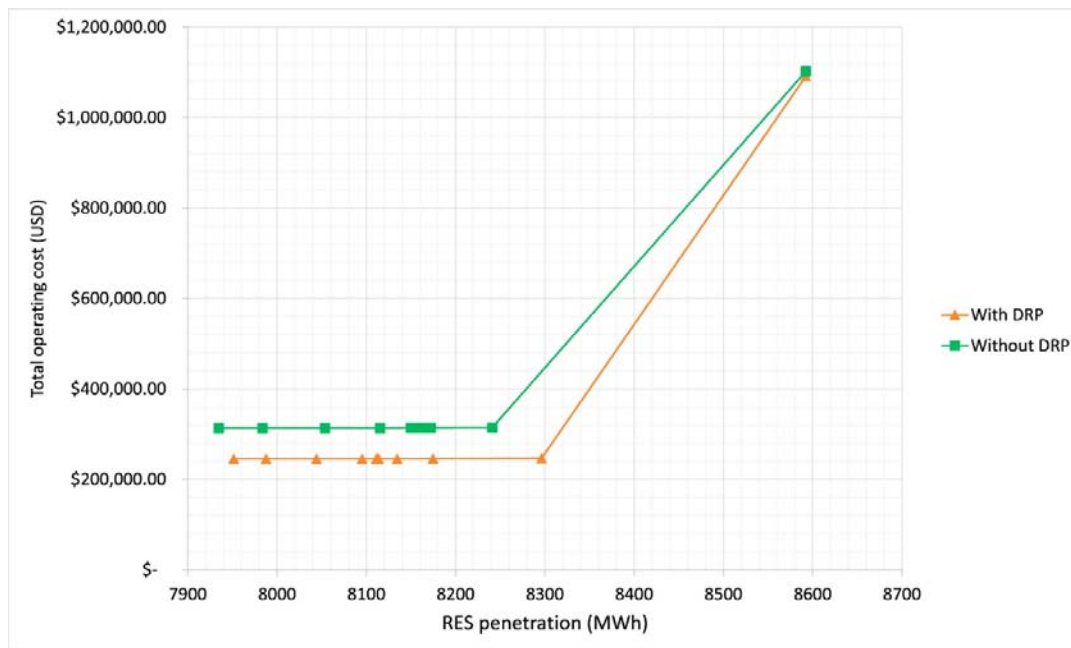


Fig. 8. Pareto front comparison between a DLC and non-DR programme.

From Fig. 8, the Pareto front curve where DRP is implemented is below the curve where there is no DLC programme. In this case, DRP is implemented to improve the system flexibility by ensuring that more RES can be injected in the power system. For the DRP Pareto front, more RES is injected at a low cost compared to the normal case without DRP. This shows that the DLC programme increases RES penetration compared to the normal RO penetration model without DLC. It also illustrates the importance of demand flexibility as an important tool to improve fluctuations in RES generation by allowing more RES penetration.

Table 7 shows a detailed comparison of the base scenario RO model and the DLC RO model.

Table 7. A comparison of base case and DRP case.

Description	Without DRP	With DRP	Delta	Perc(%)
Daily demand (MW)	26822.50	26501.30	321.20	1.19%
Thermal Gen (MWh)	18581.50	18205.00	376.50	2.03%
RES Gen (MWh)	8241.01	8296.34	-55.33	-0.67%
SR (MW)	8456.80	8424.79	32.01	0.38%
DR (MW)	0	321.20	-321.2	-
Peak RES Gen (MWh)	1774.03	1779.61	-5.58	-0.32%
Incentive (\$)	0	12844.80	-12844.8	-
TC (\$)	314,520	246,670	67850	21.57%

To analyse the influence of DRP-DLC programme on the normal RO optimisation model, this section evaluates the optimisation results as given in Table 7 which provides the optimisation results in different scenarios. According to the results in Table 7, the demand before and after RLM is shown as 321.20 MW which means that the implementation of DLC has significantly decreased the load demand. This can be seen by the thermal unit output power over the dispatch period. In the first case where no DLC is implemented, the overall thermal unit production is higher than the DLC case by 2.03%. This shows that the demand flexibility has reduced the need for an increase in thermal unit production. The same analysis can be extended to the allocation of spinning reserve requirements for the two scenarios. As clearly shown in Table 7, the base scenario has a higher requirement for spinning reserve compared to the DLC case. The introduction of DLC reduces the spinning reserve allocation by 0.38%. This leads to a reduction in the thermal unit ramping requirements as a result of managing RES penetration fluctuations. RES penetration level increase from base scenario to DLC scenario by 0.32%. This is mainly attributed by deferring load from peak period to valley period where PV production is at the highest. This is also attributed by the low energy cost of RES compared to thermal units. More importantly, the flexibility of DR has increased the RES penetration. In fact, demand flexibility is acting a temporary spinning reserve storage which in turn assists in improving network reliability and security associated with an increased RES penetration.

The overall benefit of DLC is shown by a significant decrease in the total operation cost between the two scenarios. Due to the reduced production of thermal units and minimised allocation of spinning reserves, the overall cost is also decreased for the DLC scenario. The reduction in operating cost also includes an incentive that is paid to the participating customer. The overall cost reduction is 21.57% lower than the base case scenario. These benefits are not only limited to demand reduction or the total operating cost, but also includes a significant reduction in thermal generation capacity requirements also corresponds to a reduction in power flow congestion. This ultimately increases the utilisation of RES units and it may speed up the integration of RES generators to power systems.

5.3. IEEE 118-bus test system

In this case study a large-scale power system is used to test the performance of the proposed DRP RO mode on the IEEE 118-bus system. The system base line load is found from Ref. [46] and real data from the RLM programme is used on load bus 2, 12, 18, 32 and 59. The total demand before and after the implementation of RLM is 126,854 MW and 126,830.20 MW, respectively. The sizes and

parameters of the RES generators can be found in Refs. [33] and the total installed capacity is 32,928.70 MW. The RES output power is same as the one shown in Fig. 4.

The two cases, which were studied in Sections 5.2.1 Normal operation without demand response, 5.2.2 Implementation of incentive based DRP are also performed for the large-scale system. Table 8 shows a comparison between the two cases studies. The overall performance of a large-scale test system shows no deviation from a small network since the results are consistent with previous system.

Table 8. A large-scale comparison of base case and DRP case.

Description	Without DRP	With DRP	Delta	Per (%)
Daily demand (MW)	126854	125830.2	1023.8	0.81%
Thermal Gen (MWh)	96895.69	94825.8	2069.89	2.14%
RES Gen (MWh)	29958.00	31004.48	-1046.48	-3.49%
SR (MW)	38056	37749.07	306.93	0.81%
DR (MW)	0	1023.80	-1023.8	-
Peak RES Gen (MWh)	6500	6500	0	0%
Incentive (\$)	0	40,951.20	-40,951.2	-
TC (\$)	2,288,000	1,926,400	361,600	15.80%

For example, in Table 8, the flexibility due to demand reduction is shown to increase the overall RES penetration while decreasing the production of thermal units. In total, the thermal units reduce their production by 0.89% while the RES penetration is increased by 2.14%. This is consistent with the previous test system. The reduction in thermal unit production is also followed by the reduction in spinning reserve allocation of 0.81%.

The implementation of the DLC programme has a positive impact on the operation cost. The overall operating costs are reduced by 15.8% while an incentive of \$40,951.00 is paid to participating customers. The total demand reduction before and after the RLM implementation is 1023.80 MW. Fig. 9, shows the overall demand before and after the implementation of the RLM programme. In this case study, there is no increase in RES production during peak hours as it remains the same.

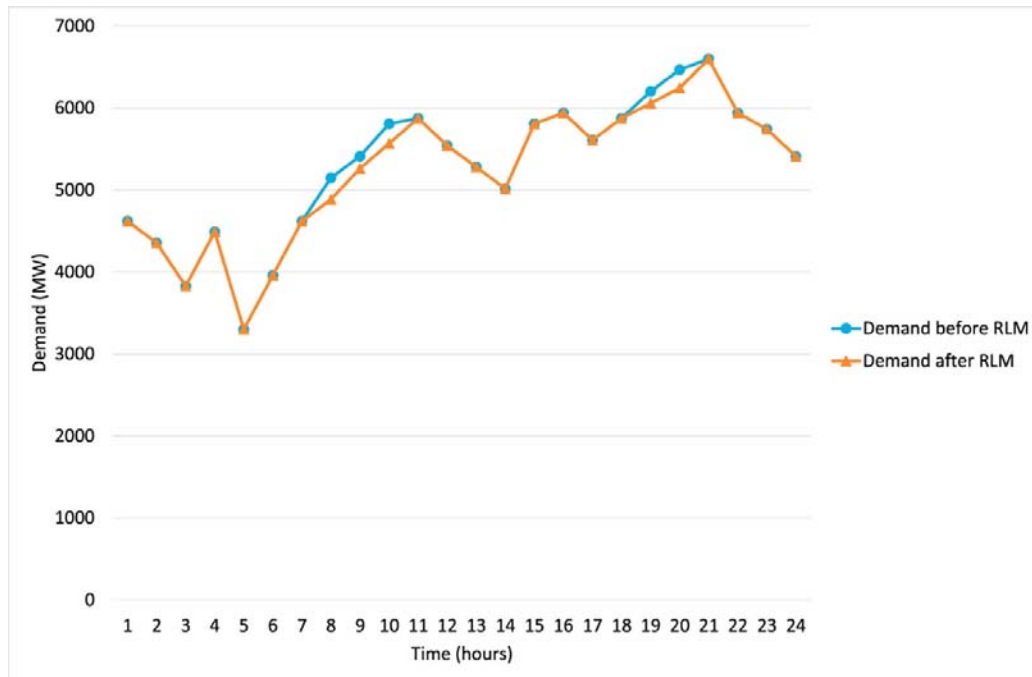


Fig. 9. Comparison of demand before and after the implementation of RLM for a large-scale network.

6. Conclusion

This paper proposes a demand response programme using direct load control of the electric water heaters. The proposed model also takes into consideration a renewable obligation framework which aims to maximise the renewable penetration level. The proposed model is tested using the standard IEEE 30-bus and 118-bus systems. The effectiveness of the model is tested using the time of use tariff structure and real time price of electricity. To show the effectiveness of the model the standard IEEE 30-bus system shows a significant increase in RES penetration while minimising the operating costs. The implementation of direct load control shows that the participating substations reduce their demand significantly to allow an increase in RES penetration especially during peak hours. Using the IEEE 30-bus system, the proposed model shows that both TOU and RTP tariff structures can be used to achieve cost saving while increasing RES penetration under direct load control. A comparative study is used to illustrate the effectiveness of the proposed model in terms of the total operating costs, peak load reduction, deferred load, spinning reserve allocation and incentive paid to participating customers. The conclusion of the study can be summarized as follows:

1. Using the standard IEEE 30-bus and 118-bus system, the proposed optimisation model shows that it can help in scheduling renewable energy sources and thermal units while allocating enough spinning reserves. The introduction of direct load control of electric water heaters on a substation level improves the level of renewable energy penetration and significantly reduces the system total operating cost.
2. Using IEEE 30-bus and 118-bus system under time of use tariff and direct load control of electric water heaters, a total cost reduction of 21.57% and 15.81% can be achieved.
3. A comparison of the normal renewable obligation model and direct load control model shows that demand response is an effective tool to achieve system reliability.

The current renewable obligation and demand response model does not take into consideration the impact of the secondary trading market for renewable obligation certificates. Therefore, the future

research will incorporate that into the model while including the supply/bid curve in modelling a multi-stage stochastic programming model for a day-ahead, adjustment and balancing market.

Credit author statement

Thabo Hlalele – Data curation, Software, Investigation, Writing – original draft preparation. Jiangfeng Zhang- Supervisor, Conceptualization, Methodology, Validation, reviewing and editing. Raj Naidoo – Supervisor, Visualization and validation. Ramesh Bansal – Supervisor, reviewing and editing.

Declaration of competing interest

The authors declare that they have no known competing financial interests or personal relationships that could have appeared to influence the work reported in this paper.

Acknowledgements

This work was supported in part by the South African National Energy Development Institute.

References

- [1] Yilmaz S, Rinaldi A, Patel M. DSM interactions: what is the impact of appliance energy efficiency measures on the demand response (peak load management)? *Energy Pol* 2020;139: 111323. <https://doi.org/10.1016/j.enpol.2020.111323>.
- [2] Mier M, Weissbart C. Power markets in transition: decarbonization, energy efficiency, and short-term demand response. *Energy Econ* 2020;86: 104644. <https://doi.org/10.1016/j.eneco.2019.104644>.
- [3] Afzalan M, Jazizadeh F. Residential loads flexibility potential for demand response using energy consumption patterns and user segments. *Appl Energy* 2019;254: 1-17.
- [4] Aghaei J, Alizadeh M-I. Demand response in smart electricity grids equipped with renewable energy sources: a review. *Renew Sustain Energy Rev* 2013;18: 64-72. <https://doi.org/10.1016/j.rser.2012.09.019>.
- [5] Yan X, Ozturk Y, Hu Z, Song Y. A review on price-driven residential demand response. *Renew Sustain Energy Rev* 2018;96: 411-419. <https://doi.org/10.1016/j.rser.2018.08.003>.
- [6] Zhou S, Shu Z, Gao Y, Gooi HB, Chen S, Tan K. Demand response program in Singapore's wholesale electricity, *Electric Power Syst. Research* 2017;142: 279-289.
- [7] Lokeshgupta B, Sivasubramani S. Multi-objective dynamic economic and emission dispatch with demand side management. *Int J Electr Power Energy Syst* 2018;97: 334-343.
- [8] Eissa MM. First time real time incentive demand response program in smart grid with i-energy management system with different resources. *Appl Energy* 2018;212: 607-621.
- [9] Khazzoom JD. Economic implications of mandated efficiency in standards for household appliances. *Energy* 1980;1: 21-40.
- [10] Borenstein S. A microeconomic framework for evaluating energy efficiency rebound and some implications. *Energy* 2015;36: 1-21.
- [11] Asadinejad A, Tomsovic K. Optimal use of incentive and price based demand response to reduce costs and price volatility. *Elec Power Syst Res* 2017;144: 215-223.
- [12] Sahebi MMR, Hosseini SH. Stochastic security constrained unit commitment incorporating demand side reserve. *Int J Elect Power Energy Syst* 2014;56: 175-184.
- [13] Mirzaei MA, Yazdankhan AS, Mohammadi-Ivatloo B. Stochastic security-constrained operation of wind and hydrogen energy storage systems integrated with price-based demand response. *Hydrogen Energy* 2019;44: 14217-14227.
- [14] Dolatabadi A, Mohammadi-Ivatloo B. The role of demand response in single and multi-objective wind-thermal generation scheduling: a stochastic programming. *Energy* 2014;64: 854-867.

- [15] Azizipanah-Abarghooee R, Golestaneh F, Gooi HB, Lin J, Bavafa F, Terzija V. Corrective economic dispatch and operational cycles for probabilistic unit commitment with demand response and high wind power. *Appl Energy* 2016;182: 634-651.
- [16] Abdi H, Dehvani E, Mohammadi F. Dynamic economic dispatch problem integrated with demand response considering non-linear responsive load models. *IEEE Trans Smart Grid* 2015;7: 2586-2595.
- [17] Lu R, Hong SH. Incentive-based demand response for smart grid with reinforcement learning and deep neural network. *Appl Energy* 2019;236: 937-949.
- [18] Nwulu NI, Xia X. Multi-objective dynamic economic emission dispatch of electric power generation integrated with game theory-based demand response programs. *Energy Convers Manag* 2015;89: 963-974.
- [19] Wang Y, Huang Y, Wang Y, Zeng M, Li F, Wang Y, Zhang Y. Energy management of smart micro-grid with response loads and distributed generation considering demand response. *J Clean Prod* 2018;197: 1069-1083.
- [20] Imani MH, Ghadi MJ, Ghavidel S, Li L. Demand response modelling in microgrid operation: a review and application for incentive-based and time-based programs. *Renew Sustain Energy Rev* 2018;94: 486-499.
- [21] Nan S, Zhou M, Li G. Optimal residential community demand response scheduling in smart grid. *Appl Energy* 2018;201: 1280-1289.
- [22] Monyei CG, Adequmi AO. Demand side management potentials for mitigating energy poverty in South Africa. *Energy Pol* 2011;111: 298-311.
- [23] Eskom IDM. Integrated demand management. 2019 [link], <https://www.eskomidm.co.za>.
- [24] Afzalan M, Jazizadeh F. Residential loads flexibility potential for demand response using energy consumption patterns and user segments. *Appl Energy* 2019;254: 113693.
- [25] Basnet SM, Aburub H, Jewell W. Residential demand response program: predictive analytics, virtual storage model and its optimization. *J Energy Storage* 2019;23: 183-194.
- [26] Kohlhepp P, Harb H, Wolisz H, Waczowicz S, Maller D, Hagenmeyer V. Large-scale grid integration of residential thermal energy storages as demand-side flexibility resource: a review of international field studies. *Renew Sustain Energy Rev* 2019;101: 527-547.
- [27] Terlouw T, AlSkaif T, Bauer C, van Sark W. Multi-objective optimization of energy arbitrage in community energy storage systems using different battery technologies. *Appl Energy* 2019;239: 356-372.
- [28] Yang S, Tan Z, Liu Z, Lin H, Ju L, Zhou F, Li J. A multi-objective stochastic optimization model for electricity retailers with energy storage system considering uncertainty and demand response. *J Clean Prod* 2020;277: 124017. <https://doi.org/10.1016/j.jclepro.2020.124017>.
- [29] Timmons D, Elahee K, Lin M. Microeconomics of electrical energy storage in a fully renewable electricity system. *Sol Energy* 2020;206: 171-180. <https://doi.org/10.1016/j.solener.2020.05.057>.
- [30] Dorotić H, Ban M, Pukšec T, Duić N. Impact of wind penetration in electricity markets on optimal power-to-heat capacities in a local district heating system. *Renew Sustain Energy Rev* 2020;132: 110095. <https://doi.org/10.1016/j.rser.2020.110095>.
- [31] Odeh RP, Watts D. Impacts of wind and solar spatial diversification on its market value: a case study of the Chilean electricity market. *Renew Sustain Energy Rev* 2019;111: 442-461. <https://doi.org/10.1016/j.rser.2019.01.015>.
- [32] O'Connell N, Pinson P, Madsen H, O'Malley M. Benefits and challenges of electrical demand response: a critical review. *Renew Sustain Energy Rev* 2014;39: 686-699.
- [33] Hlalele TG, Naidoo RM, Zhang J, Bansal RC. Dynamic economic dispatch with maximal renewable penetration under renewable obligation. *IEEE Access* 2020;8: 38794-38808.
- [34] Hlalele TG, Naidoo RM, Bansal RC, Zhang J. Multi-objective stochastic economic dispatch with maximal renewable penetration under renewable obligation. *Appl Energy* 2020;270: 115120.
- [35] Marales JM, Conejo A, Madsen H, Pinson P, Zugno M, editors. *Integrating renewables in electricity markets*. Springer; 2014.
- [36] Patel MR. *Wind and solar power systems design, analysis and operation*. Second ed. Taylor & Francis; 2006.
- [37] Zhang M, Ai X, Fang J, Yao W, Zuo W, Chen Z, Wen J. A systematic approach for the joint dispatch of energy and reserve incorporating demand response. *Appl Energy* 2018;230: 1291-1297.

- [38] Lupangu C, Bansal RC. A review of technical issues on the development of photovoltaic systems. *Renew Sustain Energy Rev* 2017;73: 950-965.
- [39] Wasa. Wind atlas for South African projects. 2020. <http://wasa.csir.co.za/web/welcome.aspx>.
- [40] SODA. Solar radiation data. <http://www.soda-pro.com/home>; 2020.
- [41] Harkouss F, Fardoun F, Biwole PH. Multi-objective optimization methodology for net zero energy buildings. *Journal of Building Engineering* 2018;16: 57-71.
- [42] Kianmehr E, Nikkhah S, Rabiee A. Multi-objective stochastic model for joint optimal allocation of DG units and network reconfiguration from DG owner's and DisCo's perspectives. *Renew Energy* 2019;132: 471-485.
- [43] Nasr M-A, Nikkhah S, Gharehpetian GB, Nasr-Azadani E, Hosseinian SH. A multi-objective voltage stability constrained energy management system for isolated microgrids. *Int J Electr Power Energy Syst* 2020;117: 105646.
- [44] de Villiers PA, van der Merwe CA. Residential load management research, Tech. rep. North-West University; 2008.
- [45] Hu F, Hughes KJ, Ingham DB, Ma L, Pourkashanian M. Dynamic economic and emission dispatch model considering wind power under energy market reform A case study. *Int J Electr Power Energy Syst* 2019;110: 184-196.
- [46] IEEE. IEEE 118 Bus data. 2020. http://motor.ece.iit.edu/data/118bus_ro.xls.
- [47] RED. Red electrica de espana, e.sios. 2020. <http://www.ree.es/en/datos/markets>.